DE GRUYTER Z. Phys. Chem. 2015; 229(4): 495–505

Jörg Sommerer and Matthias Olzmann*

Kinetics of the Reactions of Hydroxyl Radicals with Diacetylene and Vinylacetylene

Abstract: Highly unsaturated hydrocarbons like diacetylene (C_4H_2) or vinylacetylene (C_4H_4) are important intermediates in combustion that can have impact on soot formation. One of their major loss channels is reaction with hydroxyl radicals (OH). We studied the reactions C_4H_2+OH → products (1) and C_4H_4+OH → products (2) in a quasi-static reactor with helium as bath gas. The hydroxyl radicals were produced by laser flash-photolysis of nitric acid at a wavelength of 248 nm and detected by laser-induced fluorescence with excitation at 282 nm. The rate coefficients were obtained from the intensity-time profiles under pseudo-first order conditions with respect to OH. We found a virtually temperature-independent rate coefficient for reaction (1): $k_1 = (1.0 \pm 0.3) \times 10^{-11}\ \mathrm{cm^3\ s^{-1}}$ ($T = 290-670$ K, $P = 2.7-30.5$ bar) and a weakly negative temperature-dependent rate coefficient for reaction (2): $k_2(T) = (6.4 \pm 1.9) \times 10^{-12} \exp(486\ \mathrm{K}/T)\ \mathrm{cm^3\ s^{-1}}$ ($T = 295-740$ K, $P = 1.7-19.2$ bar). For neither of the two reactions pressure dependence was observed. From comparisons with analogous reaction systems, we conclude that the dominating reaction pathway is OH addition, where in the case of C_4H_4 the double bond is preferred over the triple bond.

Keywords: Reaction Kinetics, Elementary Chemical Steps, Laser-Induced Fluorescence, Diacetylene, Vinylacetylene, Hydroxyl Radicals.

DOI 10.1515/zpch-2014-0618
Received September 18, 2014; accepted October 22, 2014

Dedicated to Professor Henning Bockhorn on the occasion of his 70th birthday

---

***Corresponding author: Matthias Olzmann,** Institut für Physikalische Chemie, Karlsruher Institut für Technologie (KIT), Kaiserstr. 12, 76131 Karlsruhe, Germany, e-mail: matthias.olzmann@kit.edu
Jörg Sommerer: Institut für Physikalische Chemie, Karlsruher Institut für Technologie (KIT), Kaiserstr. 12, 76131 Karlsruhe, Germany

1 Introduction

Highly unsaturated hydrocarbons are important intermediates in fuel-rich flames [1–3]. Compounds like diacetylene (HC≡C–C≡CH, C_4H_2) and vinylacetylene (H_2C=CH–C≡CH, C_4H_4) occur in relatively high concentrations and are discussed to contribute to the formation of polycyclic aromatic hydrocarbons and soot [4–9]. C_4H_2 and C_4H_4 are mainly formed in reactions of unsaturated radicals with acetylene [4, 5, 8, 10]; one of their major loss channels is reaction with OH:

$$C_4H_2 + OH \rightarrow \text{products} \tag{1}$$

$$C_4H_4 + OH \rightarrow \text{products} \tag{2}$$

Kinetic data of these oxidation reactions are scarce.

First estimations of the rate coefficient of reaction (1) were published in 1982. Warnatz et al. [11] inferred a value of $k_1 = 5.0 \times 10^{-11}$ cm^3 s^{-1} with little or no temperature dependence from experimental investigations and numerical simulations of acetylene flames. This result was later adopted as recommendation in [12] for $T = 300-2000$ K with an estimated uncertainty of a factor of two. Bittner and Howard [13] recommended a value in the range 5×10^{-11} to 12×10^{-11} cm^3 s^{-1} from their study of benzene flames with typical temperatures between 1700 and 1900 K. At about the same time, Atkinson and Aschmann [14] measured a rate coefficient $k_1 = (1.62 \pm 0.06) \times 10^{-11}$ cm^3 s^{-1} (relative to the rate coefficient of the OH + n-butane reaction) at $T = 297$ K and atmospheric pressure. Perry [15], in a temperature-dependent study, obtained an Arrhenius expression of $k_1(T) = 1.11 \times 10^{-11} \exp[(1.7 \pm 1.3)\ \text{kJ mol}^{-1}/(RT)]\ \text{cm}^3\ \text{s}^{-1}$ from experiments conducted in the temperature range 296–688 K at pressures near 70 and 140 mbar. A value of $k_1 = (2.0 \pm 1.0) \times 10^{-11}$ cm^3 s^{-1} that is consistent with these results was obtained by Bartels et al. [16] in a discharge-flow tube study ($T = 295$ K, $P < 15$ mbar). Rate coefficients obtained from an extrapolation of the Arrhenius expression from Perry [15] were successfully used by Hidaka and coworkers [17] to model the results of their shock-tube investigation on the pyrolysis and oxidation of diacetylene.

A detailed theoretical study on the kinetics and product branching of reaction (1) was published only in 2007 by Senosiain et al. [18] These authors characterized the relevant features of the potential energy surface with high-level quantum chemical methods and calculated rate coefficients for the different product channels, using a RRKM/master-equation formalism. The resulting overall rate coefficients are essentially in agreement with the experimental values at lower temperatures but lie distinctly below the values inferred from complex kinetic modeling of shock tube and flame experiments at high temperatures. Very weak negative temperature dependence and almost no pressure dependence for pressures above ca. 25 mbar are predicted for temperatures below 500 K. To verify the calculated rate coefficients and the missing pressure dependence (which is probably due to the high-pressure limit [18]) and to supplement the measurements at lower pressures from [15], we studied reaction (1) in a similar temperature range but at higher pressures between 2 and 30 bar. In this pressure range, k_1 is safely close to its high-pressure limiting value. We determined the rate coefficient by directly monitoring the intensity of laser-induced fluorescence of OH under pseudo-first order conditions.

The situation regarding the kinetics of reaction (2) is much less satisfactory. To the best of our knowledge, there is only one estimate of the rate coefficient for the direct hydrogen abstraction reactions [4] that may become relevant at high temperatures. These values were adopted in the modeling calculations of [5] and [17]. No other kinetic data on reaction (2) are available. Therefore, we studied reaction (2) in the same way as reaction (1).

2 Experimental

The experiments were performed in a quasi-static (slow-flow) reactor with helium as the bath gas by using pulsed laser photolysis of HNO_3 for production and laser-induced fluorescence for detection of OH radicals. An excess of C_4H_2 or C_4H_4 was applied to ensure pseudo-first order conditions with respect to [OH]. Since the experimental setup was already described in detail elsewhere [19, 20], only the essentials are repeated here.

The T-shaped reaction cell with three Suprasil windows is made from stainless steel and can be heated with resistance wires up to 1000 K. The reaction mixtures were prepared in gas cylinders and were slowly flowed through the cell so as to avoid depletion of the radical precursor and accumulation of reaction products. The pressure was measured by a membrane pressure transducer suitable for pressures of up to 600 bar. The temperature in the reaction zone was determined with two thermocouples located at the inlet and outlet of the reactor. Maximum temperature differences of 20 K occurred at the highest temperatures (> 700 K) and vanished at temperatures near 300 K. Considering these differences and the location of the small reaction volume in the center between the inlet and outlet, we estimated a maximum temperature uncertainty of ±5 K at the highest temperatures.

Two windows positioned perpendicular to the gas flow at the front and back side of the reactor allow flash-photolysis of the radical precursor from one direction and resonant excitation of the radicals from the opposite direction. The fluorescence of the excited radicals was observed through a third window perpendicular to the gas flow and the laser beams. The fluorescence light was passed through a monochromator and collected in a photomultiplier tube. The electronic signal was transferred to a personal computer and analyzed. The time delay between the flash-photolysis and the detection pulse was controlled with a delay generator.

Hydroxyl radicals were obtained from photolysis of nitric acid with a KrF excimer laser at 248 nm (see [21] and [22]). The laser pulses for fluorescence excitation at 282 nm were generated by a tunable dye laser that was pumped with a XeCl excimer laser and operated with Coumarin 153 in methanol.

Nitric acid was always freshly synthesized to suppress the competing reaction of OH radicals with NO_2 from unwanted decomposition of stored liquid HNO_3. The synthesis from H_2SO_4 and $NaNO_3$ is described in [22]. Diacetylene and vinylacetylene were synthesized by dehydrohalogenation of 1,4-dichloro-2-butyne and 1,4-dichloro-2-butene, respectively, as described in [23]. Briefly, in a three-necked flask a flow of helium was passed through an alkalinized solvent (potassium hydroxide, H_2O with 10% dimethyl sulfoxide in the case of C_4H_2, ethylene glycol with 10% 2-butoxyethanol in the case of C_4H_4) that is kept at 50 °C, and the halogenated hydrocarbon was added dropwise. The product hydrocarbon formed is carried out with the helium flow and purified/isolated by passing a series of three cooling traps (−20, −80, and −200 °C, respectively), where the last one contains the clean product. This trap is then unfrozen, and the gaseous hydrocarbon is collected in a bulb. Because both C_4H_2 and C_4H_4 tend to decompose explosively, suitable safety precautions need to be taken.

Reaction mixtures were prepared manometrically in 50 liter stainless steel cylinders. The partial pressures of nitric acid, the hydrocarbon, and helium were determined with membrane pressure transducers. The freshly prepared mixtures were then allowed for at least 12 hours to mix, and the total pressure was again checked before use. The reaction mixtures were stable over several days, and no systematic change in the measured rate coefficients was observed.

3 Data analysis and results

The $C_4H_2 + OH$ reaction was investigated in the temperature range 290–670 K at pressures between 2.7 and 30.5 bar; the $C_4H_2 + OH$ reaction was studied in the temperature range 295–740 K at pressures between 1.7 and 19.2 bar. The concentrations of the hydrocarbons were varied in the ranges $(0.45–2.6) \times 10^{16}$ cm^{-3} in the case of C_4H_2 and $(1.3–10.2) \times 10^{15}$ cm^{-3} in the case of C_4H_4. The initial concentrations of HNO_3 were also in the order of 10^{16} cm^{-3} which resulted in initial

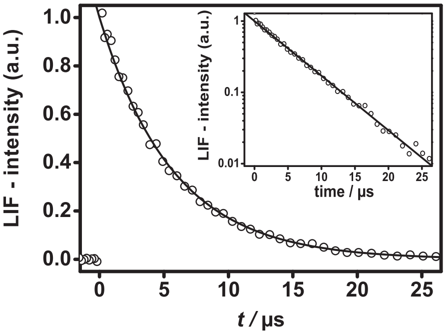

Figure 1: LIF intensity-time profile and least-squares fit for C_4H_4 + OH at $T = 370$ K, $P = 7.9$ bar, and $[C_4H_4]_0 = 7.4 \times 10^{15}$ cm^{-3}.

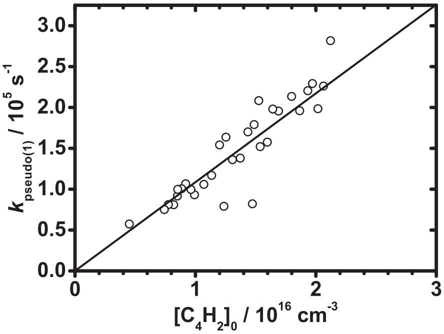

Figure 2: Plot of the pseudo-first order rate coefficient $k_{pseudo(1)}$ *vs.* $[C_4H_2]_0$ for $T = (490 \pm 8)$ K and 3 bar $< P <$ 19 bar. The linear fit through the origin gives a slope of $k_1 = 1.06 \times 10^{-11}$ cm^3 s^{-1}.

concentrations of OH in the order of 10^{12} cm^{-3} (see [21]). With such HNO_3 concentrations, competing reactions contributed less than 5% to the observed pseudo-first order rate coefficient.

For both reactions the measured fluorescence intensity-time profiles showed monoexponential decays. A typical case is displayed in Figure 1. Pseudo-first order decay constants $k_{pseudo(i)}$ ($i = 1, 2$) were obtained from the slopes of the linearized plots. We analyzed in total 150 experiments for $C_4H_2 + OH$ and 216 experiments for $C_4H_4 + OH$.

The second-order rate coefficients k_i were obtained from least-squares fits of the pseudo-first order plots $k_{pseudo(i)} = k_i[C_4H_{2i}]_0$, where we have lumped together data for a given temperature T within $T \pm 8$ K. Exemplary results are shown in Figures 2 and 3, and Arrhenius plots of the resulting rate coefficients k_1 and k_2 are given in Figures 4 and 5, respectively. For the $C_4H_2 + OH$ reaction we found

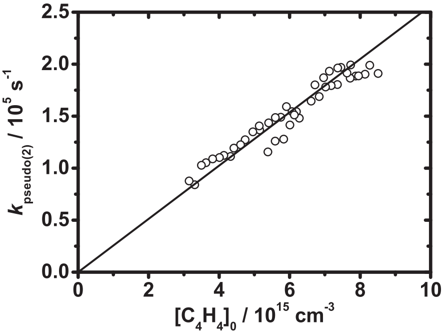

Figure 3: Plot of the pseudo-first order rate coefficient $k_{\text{pseudo}(2)}$ *vs.* $[C_4H_4]_0$ for $T = (380 \pm 8)\,K$ and $5\,\text{bar} < P < 10\,\text{bar}$. The linear fit through the origin gives a slope of $k_2 = 2.69 \times 10^{-11}\ \text{cm}^3\ \text{s}^{-1}$.

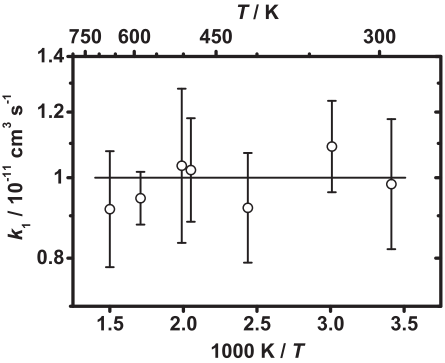

Figure 4: Arrhenius plot of the rate coefficients k_1; the data points are averages over single experiments within $T \pm 8\,K$, the error bars represent one standard deviation.

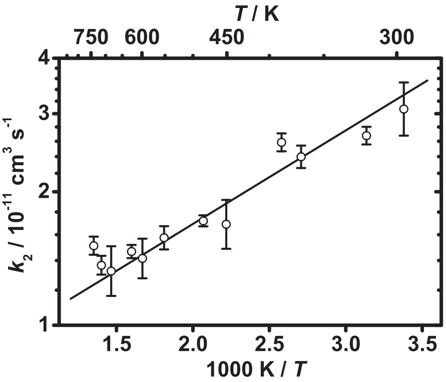

Figure 5: Arrhenius plot of the rate coefficients k_2; the data points are averages over single experiments within $T \pm 8\,K$, the error bars represent one standard deviation.

a temperature-independent rate coefficient of

$$k_1 = (1.0 \pm 0.3) \times 10^{-11}\ \mathrm{cm^3\ s^{-1}} \tag{3}$$

and for the $C_4H_4 + OH$ reaction we obtained from a least-squares fit:

$$k_2(T) = (6.4 \pm 1.9) \times 10^{-12} \exp(486\ \mathrm{K}/T)\ \mathrm{cm^3\ s^{-1}}. \tag{4}$$

Due to the multitude of parameters, which influence the uncertainty of the experiments, and which are difficult to quantify exactly, a maximum error of 30% for the rate coefficients was estimated. For neither of the two reactions a significant pressure dependence was observed.

4 Discussion

4.1 The $C_4H_2 + OH$ reaction

In Figure 6 our experimental value for k_1 is compared with results from other works. As already outlined in the introduction section, there are three more experimental studies in the temperature range of our experiments. In 1989, Bartels et al. [16] published a value of $k_1 = (2.0 \pm 1.0) \times 10^{-11}\ \mathrm{cm^3\ s^{-1}}$ ($T = 295$ K, $P < 15$ mbar) that was determined relative to the rate coefficient of n-$C_4H_{10} + OH$, for which these authors adopted an average value of $k_{\mathrm{ref}} = 3.3 \times 10^{-12}\ \mathrm{cm^3\ s^{-1}}$. Another relative rate measurement was carried out earlier by Atkinson and Aschmann [14], who obtained $k_1 = (1.62 \pm 0.06) \times 10^{-11}\ \mathrm{cm^3\ s^{-1}}$ ($T = 297$ K, $P = 967$ mbar) with a reference value of $k_{\mathrm{ref}} = 2.58 \times 10^{-12}\ \mathrm{cm^3\ s^{-1}}$ for n-$C_4H_{10} + OH$. Furthermore, Perry [15] performed a flash photolysis/resonance fluorescence study and obtained $k_1(T) = 1.11 \times 10^{-11} \exp[(1.7 \pm 1.3)\ \mathrm{kJ\ mol^{-1}}/(RT)]\ \mathrm{cm^3\ s^{-1}}$ ($T = 296-688$ K, $P = 67-133$ mbar). A detailed theoretical study was published by Senosiain et al. [18] in 2007. These authors predict a weak, negative temperature dependence for k_1 and a vanishing pressure dependence below $T = 500$ K and $P > 1$ bar.

Our experimental values of k_1 are in good agreement with the results of these earlier studies and confirm the missing pressure and temperature dependences. On an absolute scale our values are a factor of 1.5 to 2 smaller than these results, if one leaves aside the rather large estimated value from [12]. Moreover, if the more recent recommendation $k_{\mathrm{ref}} = 2.36 \times 10^{-12}\ \mathrm{cm^3\ s^{-1}}$ ($T = 298$ K) for n-$C_4H_{10} + OH$ is used [24], the values from [14] and [16] decrease to almost identical values of $k_1(T \sim 300\ \mathrm{K}) \sim 1.45 \times 10^{-11}\ \mathrm{cm^3\ s^{-1}}$ which is in still better agreement with our

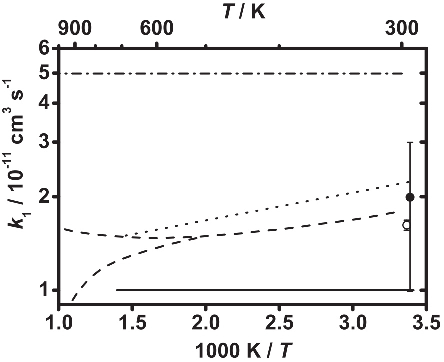

Figure 6: Arrhenius plot of rate coefficients k_1; experimental values from [16] (full circle), [14] (empty circle), and [15] (dotted line), estimation from [12] (dash-dotted line) and calculated values from [18] (dashed lines, upper branch: high-pressure limit, lower branch: $P = 1$ bar), experimental result from this work, Eq. (3) (solid line).

result. We further note that in the calculations of [18] the energy of the transition state for non-terminal OH addition to C_4H_2 was lowered by 4.2 kJ mol^{-1} to fit the cited experimental data at room temperature. A slight increase of this energy would also lead to smaller rate coefficients probably closer to our results. These calculations also show that OH addition, mainly to a terminal C atom, is the dominant reaction pathway below 1000 K.

4.2 The C_4H_4 + OH reaction

To the best of our knowledge, no information about the rate coefficient of the C_4H_4 + OH reaction is available in the literature apart from the estimation by Miller and Melius [4] on the hydrogen abstraction pathways, which are important only at high temperatures probably above 1000 K.

In contrast to C_4H_2 + OH, we observed in our experiments on C_4H_4 + OH at temperatures below 740 K a distinct, negative temperature dependence of the rate coefficient, a behavior which is typical for olefin + OH addition reactions (see e. g., [25]). Therefore, in Figure 7, we compare our results with rate coefficients of OH + C_4 olefin reactions. The similarities and differences are obvious.

Both the absolute values and the temperature dependence of k_2 is very close to the corresponding quantities of the OH + 1-butene reaction, which is a clear indication that OH addition to the double bond is the dominating reaction step for C_4H_4 + OH. We also point to the factor-of-two difference between the data for OH + 1-butene and OH + 1,3-butadiene, which is an obvious manifestation of a sta-

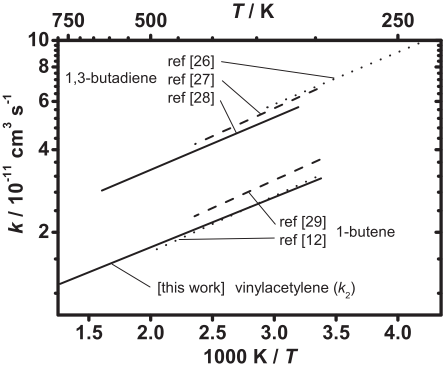

Figure 7: Arrhenius plots of rate coefficients for reactions of OH with unsaturated hydrocarbons; upper three lines: OH + 1,3-butadiene from [26] (dotted line), [27] (dashed line), and [28] (solid line); lower three lines: OH + 1-butene from [29] (dashed line) and [12] (dotted line) as well as OH + vinylacetylene from this work (solid line).

tistical factor. That is, if OH would add to both the double and the triple bond in C_4H_4 with similar rates, a larger rate coefficient close to those of the OH + diolefin reactions would result. Accordingly, our experimental finding is also in line with the observation that OH additions to terminal double bonds are faster than OH additions to the analogous triple bonds. Factors of 4 – 10 at room temperature can be inferred from literature data [25]. Further evidence for predominant addition to the double bond can be obtained from the temperature dependence. The high-pressure limiting rate coefficient of OH addition to acetylene (the most extensively studied alkyne) exhibits a clearly positive temperature dependence [30]. This is in contrast to what we observed for $C_4H_4 + OH$. Studies on larger 1-alkynes to further support this conclusion are scarce and uncertain; they indicate an at best weak temperature dependence [25]. In summary, the reactivity of C_4H_4 towards OH at temperatures below 700 K seems to resemble the reactivity of a mono-olefin.

At the highest temperatures of our experiments, near 700 K, the values of k_2 come closer to the values of k_1 (cf. Figures 4 and 5), and addition to the triple bond might come into play. On the other hand, there are indications for a turn up in the temperature dependence of k_2 in this range as can be realized from Figure 5, and hydrogen abstraction may also increasingly contribute. Unfortunately, we were not able to extend our measurements to higher temperatures to unequivocally confirm this effect. Further studies are necessary to clarify this point and to elucidate more details of the underlying reaction mechanism.

5 Summary and conclusions

The kinetics of the reactions of OH radicals with the highly unsaturated hydrocarbons diacetylene and vinylacetylene has been experimentally studied with laser photolysis/laser-induced fluorescence at temperatures between 290 and 740 K and pressures between 1.7 and 30.5 bar. In the case of $C_4H_2 + OH$ no temperature dependence of the rate coefficient was observed, and we obtained $k_1(T) = (1.0 \pm 0.3) \times 10^{-11}\ \mathrm{cm^3\ s^{-1}}$. For this reaction our study was the first performed at pressures above 1 bar. In the case of $C_4H_4 + OH$ a negative temperature dependence was found, which can be expressed in the form $k_2(T) = (6.4 \pm 1.9) \times 10^{-12} \exp(486\ \mathrm{K}/T)\ \mathrm{cm^3\ s^{-1}}$. Both rate coefficients exhibit no pressure dependence under our experimental conditions. For $C_4H_2 + OH$ the kinetic data obtained are in good agreement with results from earlier theoretical calculations and in line with results of experimental studies at lower pressures. For $C_4H_4 + OH$ no kinetic studies have been reported in the literature so far. From comparisons of our results with kinetic data of similar compounds, we conclude that the dominating steps under the conditions of our experiments for both reactions are OH additions. In the case of $C_4H_4 + OH$, addition to the double bond is likely to predominate over addition to the triple bond.

Acknowledgement: Financial support by the Deutsche Forschungsgemeinschaft (SFB 606 “Non-stationary Combustion: Transport Phenomena, Chemical Reactions, Technical Systems”) is gratefully acknowledged. We thank Isabelle Weber for help with the experiments.

References

1. K. H. Homann, M. Mochizuki, and H. Gg. Wagner, Z. Phys. Chem. Neue Folge **37** (1963) 299.
2. U. Bonne, K. H. Homann, and H. Gg. Wagner, Proc. Combust. Inst. **10** (1965) 503.
3. N. Hansen, S. J. Klippenstein, P. R. Westmoreland, T. Kasper, K. Kohse-Höinghaus, J. Wang, and T. A. Cool, Phys. Chem. Chem. Phys. **10** (2008) 366.
4. J. A. Miller and C. F. Melius, Combust. Flame **91** (1992) 21.
5. M. Frenklach and H. Wang, in: *Soot Formation in Combustion*, H. Bockhorn (Ed.), Springer, Berlin (1994), p. 165.
6. H. Wang and M. Frenklach, Combust. Flame **110** (1997) 173.
7. H. Richter and J. B. Howard, Prog. Energy Combust. Sci. **26** (2000) 565.
8. G. Blanquart, P. Pepiot-Desjardins, and H. Pitsch, Combust. Flame **156** (2009) 588.
9. A. Raman, R. Sivaramakrishnan, and K. Brezinsky, in: *Combustion Generated Fine Carbonaceous Particles*, H. Bockhorn, A. D’Anna, A. F. Sarofim, and H. Wang (Eds.), KIT Scientific Publishing, Karlsruhe (2009), p. 75.

10. A. H. Laufer and A. Fahr, Chem. Rev. **104** (2004) 2813.
11. J. Warnatz, H. Bockhorn, A. Möser, and H. W. Wenz, Proc. Combust. Inst. **19** (1982) 197.
12. J. Warnatz, in: *Combustion Chemistry*, W. C. Gardiner (Ed.), Springer, New York (1984) p. 197.
13. J. D. Bittner and J. B. Howard, Proc. Combust. Inst. **19** (1982) 211.
14. R. Atkinson and S. M. Aschmann, Combust. Flame **58** (1984) 217.
15. R. A. Perry, Combust. Flame **58** (1984) 221.
16. M. Bartels, P. Heinemann-Fiedler, and K. Hoyermann, Z. Phys. Chem. Neue Folge **161** (1989) 189.
17. Y. Hidaka, Y. Henmi, T. Ohonishi, and T. Okuno, Combust. Flame **130** (2002) 62.
18. J. P. Senosiain, S. J. Klippenstein, and J. A. Miller, Proc. Combust. Inst. **31** (2007) 185.
19. R. Forster, M. Frost, D. Fulle, H. F. Hamann, H. Hippler, A. Schlepegrell, and J. Troe, J. Chem. Phys. **103** (1995) 2949.
20. H. Hippler, F. Striebel, and B. Viskolcz, Phys. Chem. Chem. Phys. **3** (2001) 2450.
21. C. Kappler, J. Zádor, O. Welz, R. X. Fernandes, M. Olzmann, and C. Taatjes, Z. Phys. Chem. **225** (2011) 1271.
22. C. Bänsch, J. Kiecherer, M. Szöri, and M. Olzmann, J. Phys. Chem. A **117** (2013) 8343.
23. L. Brandsma, *Preparative Acetylenic Chemistry*, 2nd edn., Elsevier, Amsterdam (1988).
24. R. Atkinson, Atmos. Chem. Phys. **3** (2003) 2233.
25. R. Atkinson, J. Phys. Chem. Ref. Data Monograph **1** (1989) 1.
26. Z. Li, P. Nguyen, M. F. de Leon, J. H. Wang, K. Han, and G. Z. He, J. Phys. Chem. A **110** (2006) 2698.
27. R. Atkinson, Chem. Rev. **86** (1986) 69.
28. A. Liu, W. A. Mulac, and C. D. Jonah, J. Phys. Chem. **92** (1988) 131.
29. R. Atkinson and J. N. Pitts, Jr., J. Chem. Phys. **63** (1975) 3591.
30. J. P. Senosiain, S. J. Klippenstein, and J. A. Miller, J. Phys. Chem. A **109** (2005) 6045.